Energy Management of Electric Vehicles Aggregator Using a New Multi-Objective Algorithm

AMIN NAZARLOO[1], MOHAMMAD REZA FEYZI[2], MEHRAN SABAHI[3], AND MOHAMMAD BAGHER BANNAE SHARIFIAN[4]

[1, 2, 3, 4] *Department of Electrical and Computer Engineering, University of Tabriz, Tabriz, Iran*

Manuscript received 11 February, 2018;Revised 15 June, 2018, accepted 30 June,2018. Paper no. JEMT-1711-1046.

As regards the number of electric vehicles and their batteries energy variety in charging or discharging modes, the vehicle to grid technology can act as a variable load in charging mode or as a variable energy source in discharging mode. In this paper, a new approach is proposed. In the proposed approach, the control of the connection node voltage and the coordination of the charging and discharging of the EVs batteries are considered as the variable objective functions. The constraints are determined by several parameters such as the state of charge, connection node voltage, and charging-discharging time. Based on the proposed approach, the decision variables (which are active and reactive powers) exchanged between the EVs aggregator and the grid, are determined to achieve the defined objective functions. Reduction of grid losses in the peak load hours is the other advantage of the proposed approach. The simulations for a typical distribution system with V2G capabilities based on the proposed approach are carried out and tested for the different scenarios in charging and discharging modes. Finally, for lending credence to the proposed method, results are compared with conventional method.

keywords: *Energy Management; charging and discharging; distributed generation; grid to vehicle; peak shaving; valley filling; vehicle to grid.*

http://dx.doi.org/10.22109/jemt.2018.118868.1063

1. INTRODUCTION

One of the best future solutions to prevent the increase of fossil fuels consumption and environmental pollutions can be the extensive usage of electric vehicles (EVs). Therefore, grid overloading due to charging EVs is an important issue [1–3]. Depending on the time and the location, wherein the EVs are plugged in, they could cause overloading on the regional grid. With increasing the penetration of EVs to the grid, proper coordination between the grid and EVs is required. Uncontrolled charging of EVs may lead to voltage collapse, harmonic injection, frequency instability, and other problems in the distribution system. Therefore, it is important to coordinate and control the power flow between the grid and EVs batteries [4]. When the EVs arrive at the parking lot and connect to the grid, they receive energy and store it. EVs are also able toreturn electrical energy to the grid during peak-load, which explains the concept of the vehicle to grid (V2G) technology. The V2G operation can be defined as the provision of energy and ancillary services from EVs to the grid [5]. In order to provide the ancillary services, each EV should have some extra devices such as an electronic interface for controlling energy exchanged between the grid and EVs batteries, metering equipment, and a bidirectional communication interface to communicate with the aggregator system, which manages the charging-discharging of a high number of EVs, as are described in [6–8]. The V2G technology can also act as a supplement to the renewable energy sources, such as solar and wind energy. The electrical energy in wind and solar conditions can be stored in the batteries of EVs and returned to the grid during peak-load hours. Thus, the V2G technology effectively stabilizes intermittent power of solar and wind energy [9, 10]. Electric distribution networks considered as a critical and essential infrastructure for modern societies. So, any failure on any distribution line can cause major power outages [11]. Therefore, the V2G technology is able to increase the reliability of the network, compensate the lack of power, reduce the air pollution, improve the overall efficiency of the system, and provide the several lateral services including voltage control, frequency stability, and production of spinning reserves [12–14]. Traditionally, the electrical system infrastructure is designed to meet the highest level of demand. Therefore, the full capacity of system during low-load hours is typically underutilized. However, in the large industrial cities, the demand peak-valley gap can be as high as 40%–50% [15–18], then, peak shaving and valley filling are required to

reduce the system infrastructure cost and modify its utilization. The V2G technology, compared with other solutions can be a more efficient and economical solution to peak shaving and valley filling which reduces the gap between production and demand, certainly. Moreover, the batteries of EVs can respond to the network demand changes faster than generators (in a few seconds) [19–21]. The researchers have studied the utilization of EVs to support the grid in order to control voltage and frequency and as a distributed energy storage for peak shaving and valley filling [22–24]. In [25], battery lifetime estimation of an EV using different driving styles on arterial roads integrating recharging-scenarios in the neighborhood of the V2G integration is studied. However, voltage regulation has not been investigated. In [26], the authors have implemented the load flow to analyze the impact of charging EVs batteries on the distribution network and charging coordination between peak and low-load hours, but have not evaluated the V2G technology and charging/discharging coordination. In [27, 28], the energy storage in the EVs batteries has been discussed to meet the peak-load demands. In these researches, the authors have focused on the aggregated EVs battery energy for the transmission network, but they have not applied a proper evaluation for voltage control. In [29], the authors have presented a model of charging station of EVs to control the voltage and peak shaving using a fuzzy logic controller (FLC). Moreover, in [30], the authors have developed a multi-charging station for EVs to support the grid using the FLC method at the connection node. However, these works suffer from a poor control of the connection node voltage, especially during the charging mode. Furthermore, the FLC method is not applicable to the high number of EVs.

In this paper, considering the variable performance of the EVs batteries either as a load in charging mode or as a power supply in discharging mode a new approach is proposed to regulate the connection node voltage by controlling the power flow between the EVs and the grid. Moreover, the state of charge (SOC) of the EVs batteries is controlled in the specific margins, which are determined by vehicle's owner or aggregator. The impacts of the number of EVs that are connected to the grid are analyzed using computer simulations. The novelty of the proposed approach is the accurate regulation of the connection node voltage along with management of charging and discharging of EVs batteries which guarantees at the end of the charging and discharging process all EVs are fully charged. Moreover, the charging-discharging power, time, and the SOC of the EVs batteries are controlled within the specified limits as a deterministic setting by the EVs owners or aggregator. The proposed approach is implemented for regulating voltage in the case study of a distribution system, similar to that is used in [29]. Eventually, in order to prove the precision performance of the proposed method, results are compared with the FLC method results.

The remainder of this paper is organized as follows. Section 2 describes the concepts for problem definition such as: V2G structure and required/available energy in charging/discharging modes. Section 3 presents the problem definition. The problem formulation and its proposed solution methodology are presented in Section 4. Simulation results for three scenarios in charging and discharging modes, cost determination, and battery degradation are presented in Section 5. Finally, the findings of this work are summarized in Section 6.

2. ESSENTIAL CONCEPTS FOR PROBLEM DEFINITION

In order to define the problem and determine the objectives of the proposed method, it is required to explain some concepts related to the V2G technology.

A. The base structure of V2G

The structure of a multi-level V2G system which is shown in Fig. 1, is made up of three principal components of a charging/discharging controller, a set of aggregators, and a set of EVs. For simplicity, the aggregators that are connected directly to the EVs are called aggregator of Evs; and the aggregators that are connected to the other aggregators are called aggregator of aggregators. An aggregator of EVs can be installed in a parked position or in an area where a large number of EVs have been parked. An aggregator of aggregators can also control the several aggregators of EVs. As shown in Fig. 1, three types of the used services are defined for the power exchanging such as the charging/discharging controller-aggregator service, the aggregator-aggregator service, and the aggregator-EV service. This work is focused on the act of the charging/discharging controller-aggregator service to control the connection node voltage and the aggregator-EV service to determine the available or required energy of the EVs batteries in V2G or grid to vehicle (G2V) modes.

B. SOC-based controller for calculating required and available energy in charging and discharging modes

The V2G and G2V conditions for the EVs battery are carried out for the duration of peak and low-loads, respectively. However, some of the EVs may not have excess energy to support the grid and they may even encounter energy shortage. Therefore, this research provides a SOC-based controller. This controller adjusts each EV's battery SOC between the minimum (SOC^{min}) and the maximum (SOC^{max}) values that are determined by the vehicle's owner or aggregator. In the discharging mode, if SOC of each EV's battery is higher than SOC^{min} the excess energy can be transmitted to the grid and if it is lower than SOC^{min} , the related aggregator provides essential energy for charging the EV's battery up to SOC^{min}. On the contrary, in the charging mode the required energy is transferred from the grid to the EVs for charging the batteries up to SOC^{max}. In (1) and (2) the total available and required energies are obtained for discharging and charging modes, respectively.

$$E_{Tava} = \sum \left(SOC_i - SOC^{min} \right) \times Ec_i \quad \textbf{(1)}$$

$$E_{Treq} = \sum \left(SOC^{max} - SOC_i \right) \times Ec_i \quad \textbf{(2)}$$

where SOC_i and SOC^{max} are the current SOC and the maximum value of the SOC for a typical EV's battery, respectively. Ec_i is the energy capacity of an EV battery, E_{Tava} is the total available energy for grid support in peak-load hours, and E_{Treq} is the total required energy during charging in low-load hours.

3. PROBLEM DEFINITION

As shown in Fig. 2, a V2G system is connected to the distribution network by a 11/0.44 kV transformer and the interface line. The apparent power delivered by the EVs batteries can be obtained from:

$$S_{V2G} = V_{V2G}\, I^{*}_{V2G} \quad \textbf{(3)}$$

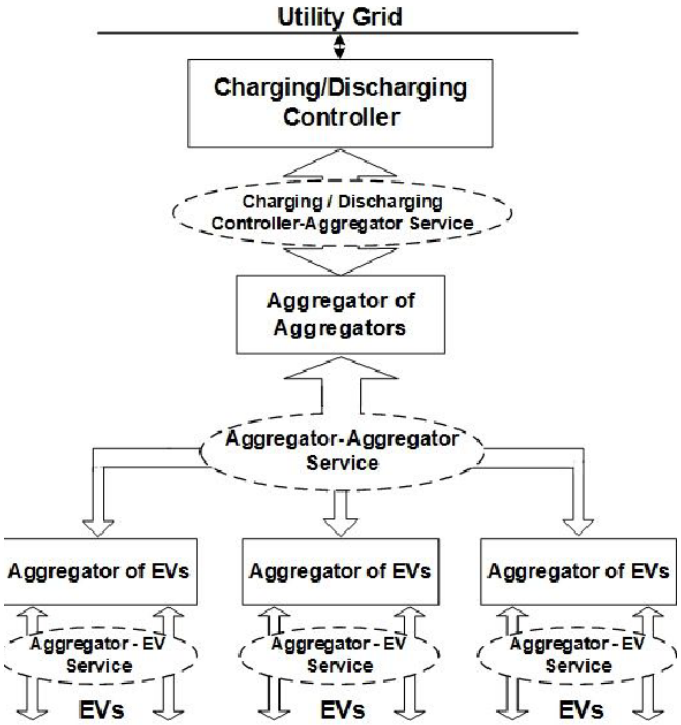

Fig. 1. The basic structure of V2G.

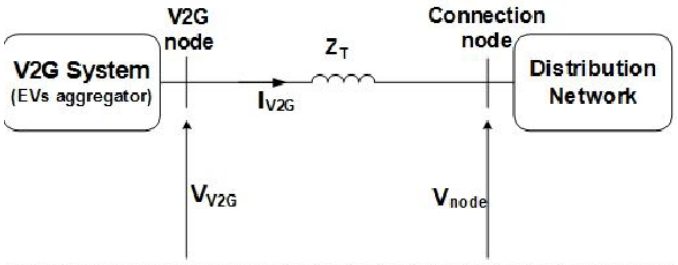

Fig. 2. Schematic diagram of a V2G system connected to the distribution network.

$$I_{V2G} = \frac{|V_{V2G}|\angle\delta - |V_{node}|\angle 0}{|Z_T|\angle\theta} \tag{4}$$

where S_{V2G} and I_{V2G} are the apparent power and the current provided by the EVs batteries, respectively. $|V_{V2G}|$ and $|V_{node}|$ are the voltage magnitudes at the V2G node and connection node, respectively. δ, θ, and $|Z_T|$ represent the phase angle between V_{V2G} and V_{node}, the phase angle of the line impedance, and the magnitude of the line impedancewhose involved in the transformer impedance, respectively. With placing (4) in (3) and separating the real and imaginary parts of the apparent power, the active power (P_{V2G}) and reactive power (Q_{V2G}) are obtained:

$$S_{V2G} = \frac{|V_{V2G}|^2}{|Z_T|}\angle\theta - \frac{|V_{V2G}| \times |V_{node}|}{|Z_T|}\angle(\delta+\theta) \tag{5}$$

$$P_{V2G} = \frac{|V_{V2G}|^2 cos(\theta) - |V_{V2G}| \times |V_{node}| cos(\theta+\delta)}{|Z_T|} \tag{6}$$

$$Q_{V2G} = \frac{|V_{V2G}|^2 sin(\theta) - |V_{V2G}| \times |V_{node}| sin(\theta+\delta)}{|Z_T|} \tag{7}$$

If only the reactive power injection by the EVs batteries is required, δ will be zero and the voltages (V_{V2G} and V_{node}) will be in phase, and the delivered active and reactive powers will be obtained as follows:

$$P_{V2G} = 0 \tag{8}$$

$$Q_{V2G} = \frac{|V_{V2G}|^2 - |V_{V2G}| \times |V_{node}|}{|X_T|} \tag{9}$$

Considering that, both of the grid power losses and the reactive feature of the loads cause the voltage drop. The phase angle must be controlled to inject the active and reactive powers into the grid to modify a high value of voltage. To modify a high value of voltage, the phase angle must be controlled to inject the active power to the grid such as reactive power. Since, in the proposed method, the grid is supported by delivering the active and reactive powers through EVs aggregator and the majority of loads in peak-load hours are also domestic types, the power factor for charging and discharging modes is assumed to be 0.9 [29]. The voltage of the V2G node is attained as [31],

$$V_{V2G}^2 = V_{node}^2 - 2\left(P_{V2G}r_T + Q_{V2G}x_T\right) + \left(\frac{P_{V2G}^2 + Q_{V2G}^2}{V_{node}^2}\right)\left(r_T^2 + x_T^2\right) \tag{10}$$

where r_T and x_T are the resistance and reactance of the interface line between the V2G node and connection node, respectively. The voltage increase due to the injection of EVs energies to the connection node can be obtained as [32]:

$$\Delta V_{V2G} = \frac{P_{V2G}r_T + Q_{V2G}x_T}{V_n} \tag{11}$$

where V_n is the line nominal voltage.

4. PROPOSED APPROACH

Fig. 3 shows a typical radial distribution system, in which a substation of 33 kV supplies the feeder of 11 kV by a 33/11 kV transformer. The primary feeder supplies various loads in sub-feeders by distribution transformers (11/0.44 kV and 500 kVA). The EVs aggregator under the V2G technology is linked to the connection node (wherein the most voltage drop occurs) by a transformer of 11/0.44 kV, 500 kVA.

In the proposed approach, the control of the connection node voltage (V_{node}) and the coordination of the charging and discharging of EVs batteries are considered as the variable objective functions. In this approach, controlling the connection node voltage as amount of 1 p.u. is considered as an initial objective function. Therefore, the active and reactive powers (which exchanged between the EVs aggregator system and the grid) are determined to achieve the initial objective function. Then, according to the duration of charging-discharging, the objective functions can be varied as one of the states presented in Table 1 based on the different situations for charging or discharging modes and the formulations for determination of the active and reactive powers are applied again to achieve the new objective functions. The predetermined objective function can be varied to the newer objective function depending on the changing or discharging conditions. For instance, from Table 1, in the state 2 of discharging mode, if connection node voltage (V_{node}) becomes equal to 1 p.u. and the charging-discharging time (TV2G) is smaller than the minimum value of the charging-discharging

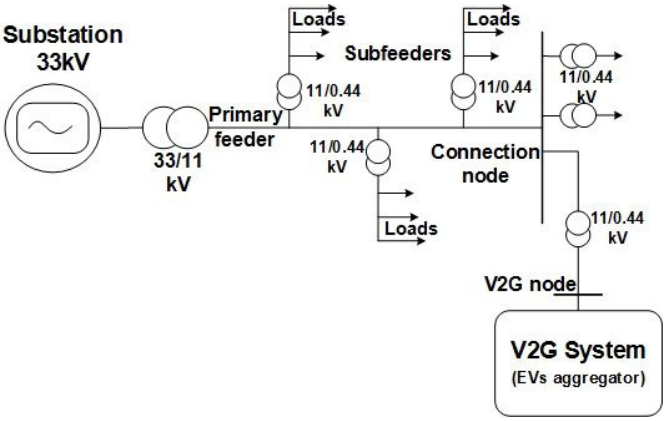

Fig. 3. Typical radial distribution system with the primary 11 kV feeder.

time (T_{V2G}^{min}). The objective functions for controlling the connection node voltage and charging-discharging time in their reference values are defined as:

$$V_{ref} < 1 \ \& \ T_{ref} = T_{V2G}^{min} \tag{12}$$

in which, V_{ref} is the reference value of the connection node voltage and T_{ref} is the reference value of charging-discharging time. It should be noted that all the situations presented in Table 1 are checked and analyzed at each step and then the appropriate objective functions are determined. Therefore, the required active and reactive powers are calculated and applied to the grid by the V2G system to achieve the desired objective function.

The constraints of the proposed approach are as follows:

$$SOC^{min} \leq SOC \leq SOC^{max} \tag{13}$$

$$T_{V2G}^{min} \leq T_{V2G} \leq T_{V2G}^{max} \tag{14}$$

$$V_{node}^{min} \leq V_{node} \leq V_{node}^{max} \tag{15}$$

In this work, the same as [29], the minimum and the maximum values of the SOC are considered 50 and 100 percent, respectively. The T_{V2G}^{min} and T_{V2G}^{max} have been determined 2 and 8 hours,

Table 1. Variable Objective Functions for Different Situations

Different situations in discharging modes

State num.	Situations	Variable Objective Function
1	$V_{PCC} = 1$, $T_{V2G}^{min} \leq T_{V2G} \leq T_{V2G}^{max}$	$V_{ref} = 1$, $T_{V2G}^{min} \leq T_{ref} \leq T_{V2G}^{max}$
2	$V_{PCC} = 1$, $T_{V2G} < T_{V2G}^{min}$	$V_{Ref} < 1$, $T_{ref} = T_{V2G}^{min}$
3	$V_{PCC} < V_{PCC}^{min}$, $T_{V2G} = T_{V2G}^{min}$	$V_{ref} = V_{PCC}^{min}$, $T_{ref} < T_{V2G}^{min}$

Different situations in charging modes

State num.	Situations	Variable Objective Function
1	$V_{node} = 1$ $T_{V2G}^{min} \leq T_{V2G} \leq T_{V2G}^{max}$	$V_{ref} = 1$ $T_{V2G}^{min} \leq T_{ref} \leq T_{V2G}^{max}$
2	$V_{node} = 1$, $T_{V2G} < T_{V2G}^{min}$	$V_{ref} > 1$, $T_{ref} = T_{V2G}^{min}$
3	$V_{node} > V_{node}^{max}$, $T_{V2G} = T_{V2G}^{min}$	$V_{ref} = V_{node}^{max}$, $T_{ref} < T_{V2G}^{min}$

respectively. The V_{node}^{min} and V_{node}^{max} are considered equal to 0.98 p.u. and 1.02 p.u., respectively. In order to achieve the specified objective functions and using the advantages of the V2G technology, the Level 2 charging system can be more appropriate than other Levels [33].

As shown in Fig. 2, I_{V2G} is the current that flows from the V2G node to the connection node and its iterative sequence is as follows:

$$I_{V2G}^{(k+1)} = \frac{V_{V2G}^{(k)} - V_{node}^{(k)}}{Z_T} \tag{16}$$

where the indexes (k) and (k+1) in the parameters imply the number of iteration. In this method, an initial voltage estimation of 1.0 + j0.0 for V2G node is satisfactory. The initial voltage of the connection node is obtained from converging the Newton-Raphson (NR) power flow solution [34] before applying the proposed approach. The voltage variation, output voltage, and the apparent, active, and reactive powers of the EVs aggregator at k+1 iteration are as follows:

$$\Delta V_{V2G}^{(k+1)} = \frac{\Delta P_{V2G}^{(k+1)} r_T + \Delta Q_{V2G}^{(k+1)} x_T}{V_n} \tag{17}$$

$$V_{V2G}^{(k+1)} = V_{V2G}^{(k)} + \Delta V_{V2G}^{(k)} \tag{18}$$

$$S_{V2G}^{(k+1)} = V_{V2G}^{(k+1)} I_{V2G}^{*(k+1)} \tag{19}$$

$$P_{V2G}^{(k+1)} = real\left\{S_{V2G}^{(k+1)}\right\} \tag{20}$$

$$Q_{V2G}^{(k+1)} = image\left\{S_{V2G}^{(k+1)}\right\} \tag{21}$$

In the proposed method, first, P_{V2G} and Q_{V2G} are computed then, through using these parameters the NR power flow is executed. However, if $Vnode$ becomes equal to V_{ref}, the obtained values in the current iteration can be used as the final amounts of the over quantities. Otherwise, the mentioned steps for the next iterations should be carried out according to (16)–(21). The iterations will continue until V_{node} becomes equal to V_{ref}; and consequently the final amounts of V_{V2G}, P_{V2G}, and Q_{V2G} are

achieved. Then, the charging-discharging time (T_{V2G}) is calculated according to:

$$T_{V2G} = \frac{E_{V2G}}{P_{V2G}} \tag{22}$$

where E_{V2G} is the available or required energy. However, if the obtained T_{V2G} satisfies its related constraint in (14), the resultant amounts of V_{V2G}, P_{V2G}, Q_{V2G}, and T_{V2G} will be selected as the final values. Otherwise, the reference value of charging-discharging time (T_{ref}) will be equal to the threshold values and V_{V2G} can be calculated as follows:

$$if \begin{cases} T_{V2G} < T_{V2G}^{min} \rightarrow T_{ref} = T_{V2G}^{min} \\ T_{V2G} > T_{V2G}^{max} \rightarrow T_{ref} = T_{V2G}^{max} \end{cases} \tag{23}$$

$$V_{V2G} = \frac{V_{node} + \left(V_{node}^2 + 4\left(\frac{Z_T \times P_{V2G}}{cos\phi}\right)\right)^{\frac{1}{2}}}{2} \tag{24}$$

However, based on the obtained values the NR power flow solver executed again. If the updated V_{node} satisfies its related constraint in (15), the obtained values will be selected as the final values. Otherwise, V_{ref} is equal to the threshold value and the other parameters are obtained as follows:

$$if \begin{cases} V_{node} < V_{node}^{min} \rightarrow V_{ref} = V_{node}^{min} \\ V_{node} > V_{node}^{max} \rightarrow V_{ref} = V_{node}^{max} \end{cases} \tag{25}$$

$$V_{V2G}^{Final} = V_{V2G} + \Delta V_{V2G} \tag{26}$$

$$P_{V2G}^{Final} = \left(\frac{\left(V_{V2G}^{Final}\right)^2 - V_{node} \times V_{V2G}^{Final}}{Z_T}\right) cos\phi \tag{27}$$

$$T_{V2G}^{Final} = \frac{E_{V2G}}{P_{V2G}^{Final}} \tag{28}$$

Therefore, the power whose exchanged between the EVs aggregator and the grid, is determined to achieve the variable objective function, satisfy the relevant constraints, make proper coordination between charging and discharging modes, and reduce grid losses during the peak-load hours. The mentioned issues for the VOF method are depicted in Fig. 4.

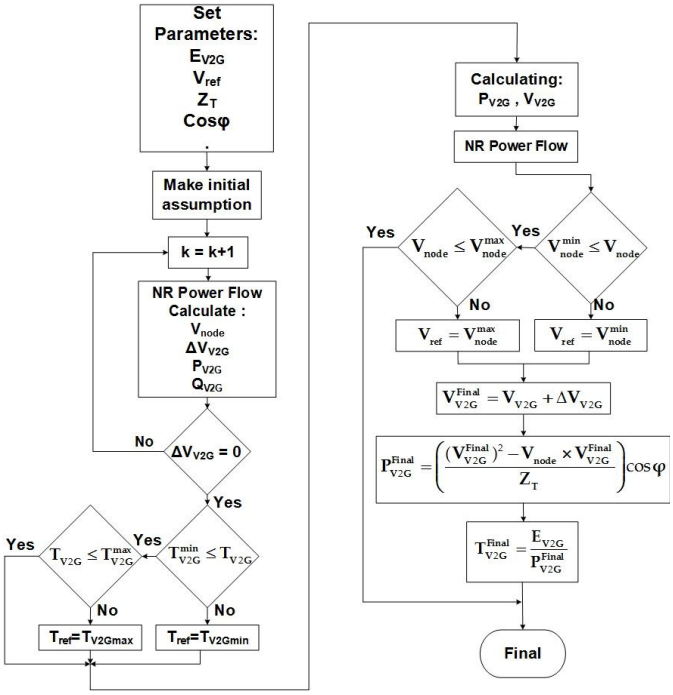

Fig. 4. Proposed method flowchart for V2G charging/discharging controller.

5. SIMULATION RESULTS AND DISCUSSIONS

To validate the proposed method, a typical radial distribution system is employed that consists of 56 nodes where 36 nodes are 11 kV and 20 nodes are 33 kV [29]. In this paper, as shown in Fig. 3, a 33 kV substation of the radial distribution system is modelled. The EVs aggregator is connected to the connection node in the distribution system, by a transformer (11/0.44 kVand 500 kVA). The transformer impedance is considered to be 0.55j p.u. The base values for apparent power and voltage are 500 kVA and 0.44 kV, respectively. Each node is decided to have 100 EVs. In this work, three types of batteries with the energy capacities of 10 kWh, 16 kWh, and 20 kWh are assumed to be used in the EVs. Due to considering the plugged-in EVs have different SOCs, the available/required energy is calculated by using the SOC-based controller. Three scenarios are developed for calculating the available energy for grid support as well as required energy for charging the EVs batteries. In the first, second, and third scenarios, the energies of 390 kWh, 192 kWh, and 99 kWh are available which are given in Tables 2, 3, and 4, respectively. These three scenarios serve as the case studies to support the grid by EVs. The corresponding assumptions are made for developing the scenarios for charging of EVs. The first, second, and third charging scenarios require the energies of 648 kWh, 435 kWh, and 305 kWh, which are given in Tables 5, 6, and 7, respectively. As shown in Fig. 3, the V2G capability has been explored for voltage control and energy management in charging and discharging modes. The simulations have been carried out for both cases of charging along with discharging of the EVs. For each case, the three scenarios have been developed.

A. Discharging Mode

By running the NR power flow solution, the connection node voltage during peak-load hours and without V2G capability is 0.93 p.u. The EVs batteries (under the V2G capability and based on the proposed method) are discharged to support the grid. Therefore, the connection node voltage improved from 0.93 p.u. to 1 p.u. after 13 iterations which are presented in Table 8. In the scenario I(as given in Table 2), the total available energy is 390 kWh. As shown in Fig. 5, the V2G system based on the proposed method has regulated the connection node voltage at 1 p.u. by

Table 2. Total available energy for grid support (scenario I)

SOC %	Capacity of Batteries kWh	No. of EVs	SOC available for grid support %	Available energy for Discharging kWh
30	10	25	-20	-50
60	16	25	10	40
90	20	50	40	400
Total available energy for discharging				390

Table 3. Total available energy for grid support (scenario II)

SOC %	Capacity of Batteries kWh	No. of EVs	SOC available for grid support %	Available energy for Discharging kWh
20	10	20	-30	-60
40	16	30	-10	-48
80	20	50	30	300
Total available energy for discharging				192

Table 8. Using the proposed approach for discharging mode

Iterations	P_{V2G} p.u.	V_{V2G} p.u.	V_{node} p.u.
1	0.1342	1.06969	0.98391
2	0.1676	1.08578	0.99137
3	0.1860	1.09441	0.99533
4	0.1960	1.09908	0.99747
5	0.2015	1.10161	0.99862
6	0.2045	1.10299	0.99925
7	0.2061	1.10374	0.99959
8	0.2070	1.10415	0.99978
9	0.2075	1.10437	0.99988
10	0.2077	1.10449	0.99993
11	0.2078	1.10456	0.99996
12	0.2079	1.10460	0.99997
13	0.2080	1.10463	1.00000

injecting the active power of 0.208 p.u. to the grid. The V2G node voltage and the discharging time are obtained 1.1046 p.u. and 3.75 hours, respectively. It is evident that T_{V2G} and V_{node} satisfy their related constraints in (14) and (15), respectively.

In scenario II, the available energy is 192 kWh and T_{V2G} is attained 1.85 hours that is lower than the minimum threshold. Therefore, in this scenario, $Tref$ is considered to be the minimum threshold. As shown in Fig. 6, P_{V2G} and V_{V2G} are respectively obtained 0.192 p.u. and 1.1061 p.u. using (22)-(24). However, the NR power flow solver is executed based on the obtained parameters. Eventually, V_{node} is obtained 0.99917 p.u. that is located in its defined constraint.

In scenario III, the available energy is 99 kWh and the T_{V2G} is attained 0.95 hours that is lower than the minimum value. Therefore, $Tref$ is considered to be the minimum threshold. As shown in Fig. 7, P_{V2G} and V_{V2G} are obtained 0.099 p.u. and 1.0572 p.u., respectively. Now, by running the NR power flow solution based on the updated values, V_{node} is obtained 0.97716 p.u. that does not satisfy the related constraint. Then, according to (25), V_{ref} is assumed to be V_{node}^{min}. by using (26)-(28), V_{V2G}, P_{V2G}, and T_{V2G} are obtained 1.06 p.u., 0.1369 p.u., and 1.43 hours, respectively. Finally, by running the NR power flow solution again, V_{node} is attained 0.9816 p.u. that fulfills its related constraint. As presented in Table 9, the active and reactive power

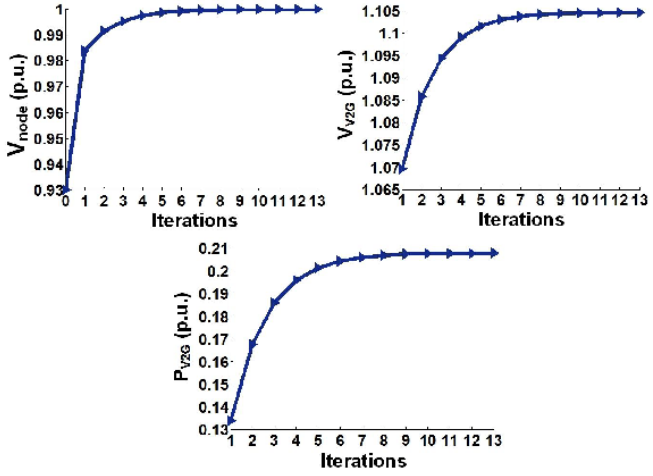

Fig. 5. V_node without (Iteration 0) and with the V2G controller, V_{V2G}, and PV2G of the proposed method in each iteration in the scenario I.

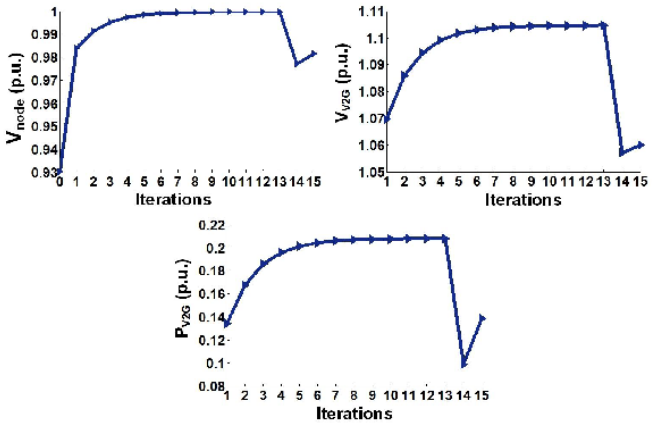

Fig. 6. V_node without and with the V2G controller, V_{V2G}, and PV2G of the proposed method in each iteration in the scenario II.

losses have been respectively decreased by 18.14% and 19% in the scenario I, and 13.2% and 14% in the other scenarios.

By discharging the EVs batteries, their SOC levels are also

Table 4. Total available energy for grid support (scenario III)

SOC %	Capacity of Batteries kWh	No. of EVs	SOC available for grid support %	Available energy for Discharging kWh
27	10	30	-23	-69
35	16	30	-15	-72
80	20	40	30	240
Total available energy for discharging				99

Table 5. Total required energy during charging (scenario I)

SOC %	Capacity of Batteries kWh	No. of EVs	SOC required for charging %	Required energy for charging kWh
30	10	25	70	175
60	16	25	40	160
90	20	50	10	100
Total required energy for charging				435

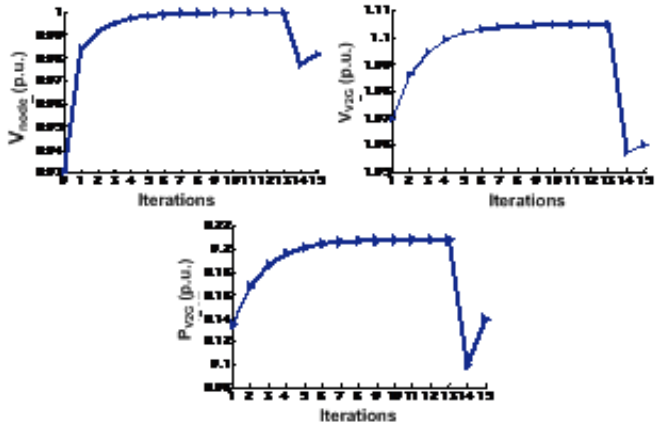

Fig. 7. V_{node} without and with the V2G controller, V_{V2G}, and PV2G of the proposed method in each iteration in the scenario III.

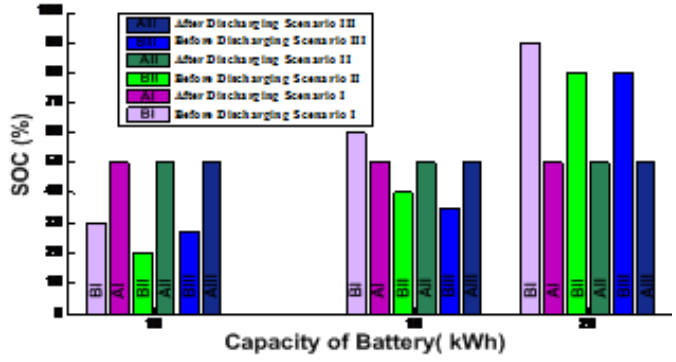

Fig. 8. SOC of EVs battery before and after discharging.

changed. The SOC levels of the EVs batteries (before and after discharging) are shown in Fig. 8. As shown, the proposed approach always ensures that the batteries SOC level is maintained at least on 50% during discharging mode. As shown in the simulation results, the proposed approach has successfully managed the available/required energy of EVs batteries to support the grid, control the connection node voltage, and reduce the grid losses.

Table 10. Using proposed approach for charging mode

Iterations	P_{V2G} p.u.	Q_{V2G} p.u.	V_{node} p.u.
1	-0.0361	-0.0175	1.0129
2	-0.0581	-0.0281	1.0080
3	-0.0714	-0.0346	1.0049
4	-0.0795	-0.0385	1.0030
5	-0.0844	-0.0409	1.0018
6	-0.0873	-0.0423	1.0011
7	-0.0891	-0.0431	1.0007
8	-0.0902	-0.0437	1.0004
9	-0.0908	-0.0440	1.0003
10	-0.0913	-0.0442	1.0002
11	-0.0916	-0.0444	1.0001
12	-0.0918	-0.0445	1.0000

B. Charging mode

The EVs that require energy for charging their batteries are developed in three scenarios. The connection node voltage during low-load hours and without V2G capability is 1.021 p.u.. As presented in Table 10, due to the charging of EVs batteries through using the proposed method, the connection node voltage is reduced to 1 p.u. after 12 iterations. In Table 10, the negative values of the active and reactive powers indicate a change in power flow direction from the grid to the EVs aggregator.

In the scenario I, the required energy to charge the EVs batteries in low-load hours is 648 kWh. As shown in Fig. 9, the power which is drawn from the grid obtained 0.0918 p.u. (at the 12th iteration). The duration of charging EVs is attained 14.12 hours that does not satisfy its related constraint in (14). Therefore, the T_{ref} is considered to be the maximum threshold. So, the active and reactive powers are calculated and obtained 0.162 and 0.0785 p.u., respectively. By running the NR power flow solution, Vnode is achieved 0.98135 p.u. that is placed in its related constraint in (15).

In scenario II, the required energy to charge the EVs batteries is 435 kWh, and the charging duration is achieved 9.48 hours whose is higher than the maximum threshold. Therefore, T_{ref} considered to be the maximum threshold. As shown in Fig. 10, the active and reactive powers which are drawn from the grid achieved 0.1088 and 0.0527 p.u., respectively. Then, by running

Table 6. Total required energy during charging (scenario II)

SOC %	Capacity of Batteries kWh	No. of EVs	SOC required for charging %	Required energy for charging kWh
20	10	20	80	160
40	16	30	60	288
80	20	50	20	200
Total required energy for charging				648

Table 7. Total required energy during charging (scenario III)

SOC %	Capacity of Batteries kWh	No. of EVs	SOC required for charging %	Required energy for charging kWh
65	10	30	35	105
75	16	30	25	120
90	20	40	10	80
Total required energy for charging				305

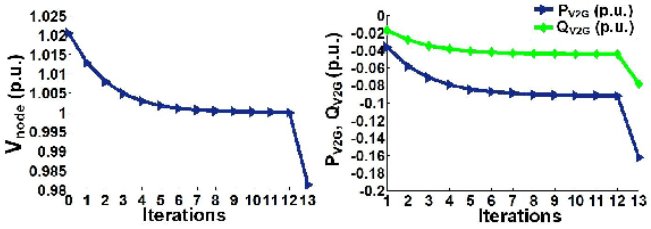

Fig. 9. V_{node} without (Iteration 0) and with the V2G controller, P_{V2G}, and Q_{V2G} of the proposed method in each iteration in the scenario I.

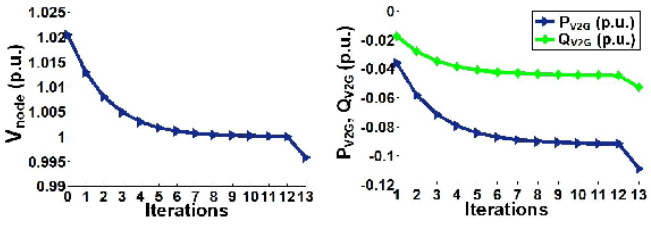

Fig. 10. V_{node} without and with the V2G controller,P_{V2G}, and Q_{V2G} of the proposed method in each iteration in the scenario II.

NR power flow for the updated power values, V_{node} obtained 0.9958 p.u. (it is very close to 1 p.u.) and satisfies the related constraint. In scenario III, the required energy to charge the EVs batteries is 305 kWh and the charging time is achieved 6.65 hours which satisfies its related constraint. Therefore, as shown in Fig. 11, the EVs aggregator provides the required energy to charge the EVs batteries for 6.65 hours duration, and controls V_{node} at 1 p.u. by getting the active and reactive powers from the grid (0.0918 and 0.0445 p.u. respectively). Through charging the EVs batteries, their SOCs level has been changed. The SOCs of the EVs batteries before and after charging are shown in Fig. 12. As shown, the batteries SOCs are increased until all of the batteries are fully charged during the charging scenarios.

As the load changes, the required power of V2G controlled by changing the power flow between grid and batteries. Therefore,

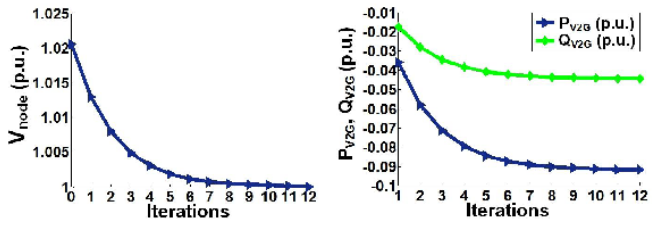

Fig. 11. V_{node} without and with the V2G controller,P_{V2G}, and Q_{V2G} of the proposed method in each iteration in the scenario III.

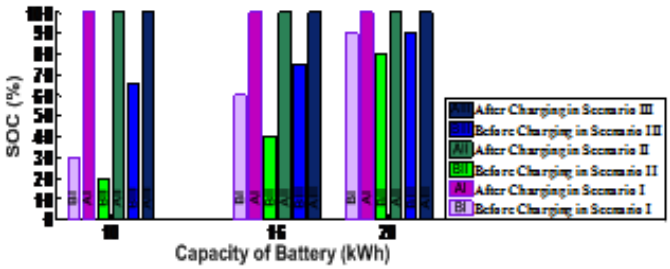

Fig. 12. SOC of EV$_s$ battery before and after charging.

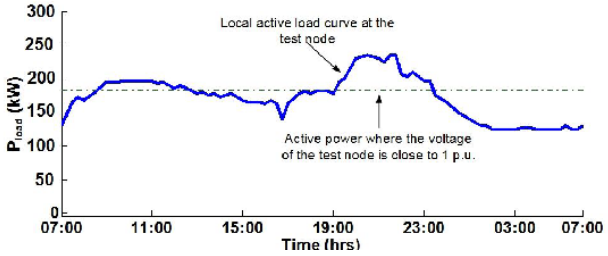

Fig. 13. Local load curve at the connection node without V2G technology.

the load profile of the connection node improved as well as the peak shaving and valley filling.

Aim to prove the versatility, the proposed method has been compared with the conventional FLC method in first and second scenarios. These comparisons for both of discharging and

Table 9. Grid losses with/without V2G in peak hours

All in p.u.	Without V2G system	With V2G system		
		Scenario I	Scenario II	Scenario III
Active Power Losses	0.45452	0.37206	0.39449	0.39539
Reactive Power Losses	1.5804	1.28	1.3593	1.3592

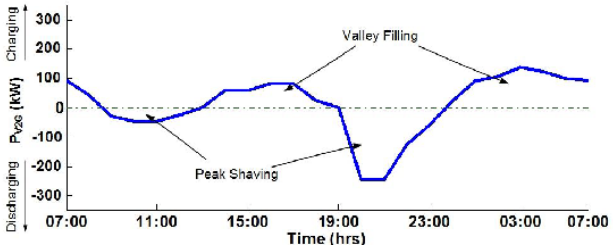

Fig. 14. Power flow between the grid and the EVs batteries.

charging modes are presented in Tables 11 and 12, respectively. Therefore, as shown, the proposed method is able to coordinate the charging and discharging of the EVs batteries, support the grid, and control the connection node voltage, perfectly.

C. Cost determination and battery degradation

The battery degradation is a function of SOC, ambient temperature, charging time, Depth of Discharge (DOD), charge/discharge rate, and the cycles number [35]. The power company has set three different tariffs for low, normal, and peak load hours to sell electrical energy to customers in G2V mode [36]. In the G2V mode, the cost of electric energy consumed by EVs is as follows:

$$C^{G2V} = \sum_{i=1}^{24} \alpha_i E_i^{G2V} \tag{29}$$

in which C^{G2V} is the total cost of electric energy used by EVs in 24 hours. α_i and E_i^{G2V} are the energy tariffs per kilowatt-hour and the amount of energy consumed by EVs in the i^{th} time, respectively. Similarly, the EVs owners can also take different tariffs for low, normal, and peak load hours for the sale of energy to the grid. Therefore, in the V2G mode, the proceeds from the sale of energy to the grid by the owners of EVs can be obtained as follows:

$$C^{V2G} = \sum_{i=1}^{24} \beta_i E_i^{V2G} \tag{30}$$

in which, C^{V2G} is the total revenue from the sale of energy to the grid by EVs owners within 24 hours. β_i and E_i^{V2G} are the different energy sale tariffs and the amounts of energy transferred to the grid in the i^{th} time, respectively. In order to economize the V2G technology based on the proposed method, the revenue which obtained from the sale of energy to the grid by EVs owners can be more or equal to the sum of the cost of purchasing energy from the grid by the owners and cost of the battery degradation.

$$C^{V2G} \leq C^{G2V} + C_{BAT}^{DEG} \tag{31}$$

where C_{BAT}^{DEG} is the cost of the battery degradation for energy that exchanged between the grid and EVs during 24 hours and

Table 11. Comparison of the proposed method with FLC method in discharging mode

Scenarios	Methods	P_{V2G} kW	T_{V2G} Hours	V_{node} p.u.
I E_{V2G} = 390 kWh	Proposed	104	3.75	1
	FLC	104	3.75	0.98
II E_{V2G} = 192 kWh	Proposed	96	2	0.99917
	Proposed	70	2.74	0.98738
	FLC	70	2.47	0.95 < 0.98

can be described as:

$$C_{BAT}^{DEG} = \sum_{j=1}^{n_{EV}} \gamma_j \times E_j^{TOT} \tag{32}$$

in which E_j^{TOT} and n_{EV} are the total energy exchanged between the grid and j^{th} EV, and the number of all EVs connected to the grid, respectively. γ_j is the j^{th} EV battery degradation factor for a kilowatt-hour energy exchange and can be defined as follows:

$$\gamma_j = \frac{BATP_j}{2 \times E_j^{cap} \times L_J^{cyc}} \tag{33}$$

where $BATP_j$ and E_j^{cap} are the battery price and the nominal energy capacity of j^{th} EV battery, respectively. L_{cyc} is the j^{th} EV battery life cycle in terms of charging-discharging cycles.

In the G2V mode, the power company applies the tariff for energy consumption at the low load hours to reduce half of the normal load tariff and at the peak load hours to double increase of the normal load tariff. Therefore, in V2G mode, for determining the sale of the energy tariffs, it is possible to set the tariff at low load hours to half of the normal load tariff and at peak load hours to double of the normal load tariff.

$$\begin{cases} \alpha_1 = \alpha/2 \\ \alpha_2 = \alpha \\ \alpha_3 = 2\alpha \end{cases} ; \begin{cases} \beta_1 = \beta/2 \\ \beta_2 = \beta \\ \beta_3 = 2\beta \end{cases} ; \begin{cases} BATP_1 = \rho \\ BATP_2 = 2\rho \\ BATP_3 = 3\rho \end{cases} \tag{34}$$

For instance, scenario II involved in charging and discharging modes by substituting the values of energy exchanged between the grid and EVs, the related tariffs, and assumptions of (34) in (31). So, the following result is obtained:

$$\beta \leq 0.844\alpha + 1.2 \times 10^{-4}\rho \tag{35}$$

Therefore, according to (35), the owners of EVs using V2G technology based on the proposed method can obtain a net profit without paying for purchasing and charging the battery. However, some governments determine subsidies for the use of V2G technology, which leads to a further increase in the owners' profits.

Table 12. Comparison of the proposed method with FLC method in charging mode

Scenarios	Methods	P_{G2V} kW	T_{G2V} Hours	V_{node} p.u.
I E_{V2G} = 648 kWh	Proposed	81	8	0.98135
	FLC	170	3.81	0.963 < 0.98
II E_{V2G} = 435 kWh	Proposed	54.4	8	0.9958
	Proposed	60	7.25	0.99292
	FLC	60	7.25	0.91 < 0.98

6. CONCLUSION

In this work, as regards the variability feature of EVs batteries, either as a load or as an energy source a new approach is proposed in which the objective function is variable. In the proposed approach, the adjustment of the connection node voltage and the coordination of the charging and discharging of EVs batteries are considered as the variable objective functions. The constraints of the proposed approach are the batteries SOC, the connection node voltage, and the charging/discharging time. The active and reactive power flows are controlled to achieve the specified objective functions and using the advantages of the V2G technology. A typical radial distribution system has been modeled to demonstrate the V2G capabilities such as supporting the grid in peak-load hours and reducing the voltage fluctuations. The simulation results lend credence to the versatility of the proposed approach in the proper performance of the grid by controlling the connection node voltage, reducing the grid losses in the peak-load hours, and coordinating the charging and discharging of EVs batteries.

REFERENCES

1. W. Kempton and J. Tomić, "Vehicle-to-grid power fundamentals: Calculating capacity and net revenue," *Journal of power sources*, vol. 144, no. 1, pp. 268–279, 2005.
2. E. L. Karfopoulos and N. D. Hatziargyriou, "Distributed coordination of electric vehicles providing v2g services," *IEEE Transactions on Power Systems*, vol. 31, no. 1, pp. 329–338, 2016.
3. A. Y. Lam, K.-C. Leung, and V. O. Li, "Capacity estimation for vehicle-to-grid frequency regulation services with smart charging mechanism," *IEEE Transactions on Smart Grid*, vol. 7, no. 1, pp. 156–166, 2016.
4. Y. Fan, W. Zhu, Z. Xue, L. Zhang, and Z. Zou, "A multi-function conversion technique for vehicle-to-grid applications," *Energies*, vol. 8, no. 8, pp. 7638–7653, 2015.
5. H. V. Haghi and Z. Qu, "A kernel-based predictive model of ev capacity for distributed voltage control and demand response," *IEEE Transactions on Smart Grid*, 2016.
6. J. Donadee and M. D. Ilić, "Stochastic optimization of grid to vehicle frequency regulation capacity bids," *IEEE Transactions on Smart Grid*, vol. 5, no. 2, pp. 1061–1069, 2014.
7. M. Ansari, A. T. Al-Awami, E. Sortomme, and M. Abido, "Coordinated bidding of ancillary services for vehicle-to-grid using fuzzy optimization," *IEEE Transactions on Smart Grid*, vol. 6, no. 1, pp. 261–270, 2015.
8. A. K. Srivastava, B. Annabathina, and S. Kamalasadan, "The challenges and policy options for integrating plug-in hybrid electric vehicle into the electric grid," *The Electricity Journal*, vol. 23, no. 3, pp. 83–91, 2010.
9. R. Sioshansi and P. Denholm, "Emissions impacts and benefits of plug-in hybrid electric vehicles and vehicle-to-grid services," *Environmental science & technology*, vol. 43, no. 4, pp. 1199–1204, 2009.
10. J. R. Pillai and B. Bak-Jensen, "Integration of vehicle-to-grid in the western danish power system," *IEEE Transactions on Sustainable Energy*, vol. 2, no. 1, pp. 12–19, 2011.
11. M. H. Tushar and C. Assi, "Volt-var control through joint optimization of capacitor bank switching, renewable energy, and home appliances," *IEEE Transactions on Smart Grid*, 2017.
12. B. K. Sovacool and R. F. Hirsh, "Beyond batteries: An examination of the benefits and barriers to plug-in hybrid electric vehicles (phevs) and a vehicle-to-grid (v2g) transition," *Energy Policy*, vol. 37, no. 3, pp. 1095–1103, 2009.
13. H. Turton and F. Moura, "Vehicle-to-grid systems for sustainable development: An integrated energy analysis," *Technological Forecasting and Social Change*, vol. 75, no. 8, pp. 1091–1108, 2008.
14. A. Y. Saber and G. K. Venayagamoorthy, "Intelligent unit commitment with vehicle-to-grid—a cost-emission optimization," *Journal of Power Sources*, vol. 195, no. 3, pp. 898–911, 2010.
15. W. Kempton and J. Tomić, "Vehicle-to-grid power implementation: From stabilizing the grid to supporting large-scale renewable energy," *Journal of power sources*, vol. 144, no. 1, pp. 280–294, 2005.
16. S. Han, S. H. Han, and K. Sezaki, "Design of an optimal aggregator for vehicle-to-grid regulation service," in *Innovative Smart Grid Technologies (ISGT), 2010*, pp. 1–8, IEEE, 2010.
17. U. K. Madawala and D. J. Thrimawithana, "A bidirectional inductive power interface for electric vehicles in v2g systems," *IEEE Transactions on Industrial Electronics*, vol. 58, no. 10, pp. 4789–4796, 2011.
18. Z. Wang and S. Wang, "Grid power peak shaving and valley filling using vehicle-to-grid systems," *IEEE Transactions on power delivery*, vol. 28, no. 3, pp. 1822–1829, 2013.
19. E. Sortomme and M. A. El-Sharkawi, "Optimal combined bidding of vehicle-to-grid ancillary services," *IEEE Transactions on Smart Grid*, vol. 3, no. 1, pp. 70–79, 2012.
20. M. Singh, K. Thirugnanam, P. Kumar, and I. Kar, "Real-time coordination of electric vehicles to support the grid at the distribution substation level," *IEEE Systems Journal*, vol. 9, no. 3, pp. 1000–1010, 2015.
21. A. Kavousi-Fard, T. Niknam, and M. Fotuhi-Firuzabad, "Stochastic reconfiguration and optimal coordination of v2g plug-in electric vehicles considering correlated wind power generation," *IEEE Transactions on Sustainable Energy*, vol. 6, no. 3, pp. 822–830, 2015.
22. S. Han, S. Han, and K. Sezaki, "Development of an optimal vehicle-to-grid aggregator for frequency regulation," *IEEE Transactions on smart grid*, vol. 1, no. 1, pp. 65–72, 2010.
23. C. Wu, H. Mohsenian-Rad, and J. Huang, "Vehicle-to-aggregator interaction game," *IEEE Transactions on Smart Grid*, vol. 3, no. 1, pp. 434–442, 2012.
24. E. Sortomme and M. A. El-Sharkawi, "Optimal scheduling of vehicle-to-grid energy and ancillary services," *IEEE Transactions on Smart Grid*, vol. 3, no. 1, pp. 351–359, 2012.
25. M. Jafari, A. Gauchia, S. Zhao, K. Zhang, and L. Gauchia, "Electric vehicle battery cycle aging evaluation in real-world daily driving and vehicle-to-grid services," *IEEE Transactions on Transportation Electrification*, vol. 4, no. 1, pp. 122–134, 2018.
26. K. Clement-Nyns, E. Haesen, and J. Driesen, "The impact of charging plug-in hybrid electric vehicles on a residential distribution grid," *IEEE Transactions on power systems*, vol. 25, no. 1, pp. 371–380, 2010.
27. Y. Ota, H. Taniguchi, T. Nakajima, K. M. Liyanage, J. Baba, and A. Yokoyama, "Autonomous distributed v2g (vehicle-to-grid) satisfying scheduled charging.," *IEEE Trans. Smart Grid*, vol. 3, no. 1, pp. 559–564, 2012.
28. Y. Ma, T. Houghton, A. Cruden, and D. Infield, "Modeling the benefits of vehicle-to-grid technology to a power system," *IEEE Transactions on power systems*, vol. 27, no. 2, pp. 1012–1020, 2012.
29. M. Singh, P. Kumar, and I. Kar, "Implementation of vehicle to grid infrastructure using fuzzy logic controller," *IEEE Transactions on Smart Grid*, vol. 3, no. 1, pp. 565–577, 2012.
30. M. Singh, P. Kumar, and I. Kar, "A multi charging station for electric vehicles and its utilization for load management and the grid support," *IEEE Transactions on Smart Grid*, vol. 4, no. 2, pp. 1026–1037, 2013.
31. M. E. Baran and F. F. Wu, "Network reconfiguration in distribution systems for loss reduction and load balancing," *IEEE Transactions on Power delivery*, vol. 4, no. 2, pp. 1401–1407, 1989.
32. N. Jenkins, R. Allan, P. Crossley, D. Kirschen, and G. Strbac, "Technical impacts of embedded generation on the distribution system," *Embed-*

ded generation, pp. 11–12, 2000.
33. S. Habib, M. M. Khan, F. Abbas, L. Sang, M. U. Shahid, and H. Tang, "A comprehensive study of implemented international standards, technical challenges, impacts and prospects for electric vehicles," *IEEE Access*, 2018.
34. G. Andersson, "Power system analysis-power flow analysis fault analysis power system dynamics and stability," *Relatório té, ETH Zurich*, 2012.
35. A. Ahmadian, M. Sedghi, B. Mohammadi-ivatloo, A. Elkamel, M. A. Golkar, and M. W. Fowler, "Cost-benefit analysis of v2g implementation in distribution networks considering pevs battery degradation," *IEEE Transactions on Sustainable Energy*, 2017.
36. A. Nazarloo, M. R. Feyzi, M. Sabahi, and M. BANNAE SHARIFIAN, "Improving voltage profile and optimal scheduling of vehicle to grid energy based on a new method," *Advances in Electrical And Computer Engineering*, vol. 18, no. 1, pp. 81–88, 2018.